# Evaluating the Multifactorial Effects on SARS-CoV-2 Spread in Tokyo Metropolitan Area with an Agent-Based Model

Jianing Chu[a] and Yu Chen[b]
*SCS Laboratory, The University of Tokyo, Kashiwanoha 5-1-5, Chiba, Japan*

Abstract: The eighth wave of Coronavirus infection in Tokyo hit high records in December 2022. This paper aims to build a Tokyo-based down-scaled simulation environment to explain the eight epidemic trends using agent-based modelling and extended SEIR denotation. Four key factors are examined in this research, that are: 1. Vaccination, 2. Virus mutation, 3. Government policy and 4. PCR test. Our investigation uncovers that the reported cases during the eight epidemic waves represent merely a fraction of the true extent of infections. Additionally, our study innovates by simulating the decline of antibodies at the individual level. Our study also innovates in combining agent-based modelling and extended SEIR modelling to simulate eight continuous epidemic waves in Tokyo, considering circumstances like Olympics, state of emergency declaration, traveling policies etc. Upon analyzing the simulated outcomes, we observe a correlation between the onset of new epidemic waves and the decrease in the population possessing antibodies. Our simulation further indicates the necessity for aligning the level of PCR testing with the available medical resources. Finally, by comparing the simulation results with actual data for the eighth wave, we forewarned of a potential resurgence in the epidemic during May and June 2023.

## 1 INTRODUCTION

On May 8, 2023, a significant measure was taken in Japan as the government downgraded COVID-19 from a class 2 infectious disease to a class 5 disease, marking a pivotal moment in the country's fight against the virus. This reclassification signifies a shift in the severity and risk assessment of COVID-19 in Japan, prompting a re-evaluation of public health policies and strategies. This paper specifically focuses on the critical contribution of epidemiology in the context of SARS-CoV-2 in Japan, aiming to shed light on its vital role in advancing global health objectives during the ongoing COVID-19 pandemic.

At the initiation of our study, we posit that the epidemic trend is chiefly shaped by four aspects: vaccination; virus mutation; government policy, and PCR testing. This assumption is grounded in the following considerations: 1) vaccination plays a crucial role in generating antibodies, thereby curbing the spread of the Coronavirus; 2) mutations in the

Table 1: Summary of agents' health status.

| States | Meanings |
| --- | --- |
| S1 | Susceptible, healthy, no antibody or vaccination |
| E | Exposed, within the infection range to I1 |
| I1 | Infected, unconfirmed and not tested |
| I2 | Infected, confirmed via PCR test |
| V | Healthy, vaccinated, possess antibody |
| R | Healthy, cured, possess antibody |
| S2 | Healthy, susceptible, vaccinated, lose antibody |
| D | Dead |

virus can potentially enhance its transmissibility by evading immunity; 3) government policies, such as travel restrictions, aim to mitigate the spread of the virus; and 4) the adequacy of PCR testing capacity significantly influences the tally of confirmed cases.

This study utilizes an extended SEIR framework (refer to Table 1) along with the construction of an

[a] https://orcid.org/0009-0009-0495-1376
[b] https://orcid.org/0000-0002-7075-2457

agent-based model. Further elaboration on these methods will be presented in Sec. 3. The actual data pertaining to the four factors mentioned are sourced from the Tokyo Metropolitan Government and will be utilized for model validation. Our primary objective is to replicate the onset, peak, decline, and maximum daily infection rates of each wave. In continuation of our previous study (Chu et al., 2023), our goal is to not only explain the occurrence of the eight waves but to simulate possible infectious diseases in the future.

The paper is structured as follows: Firstly, we review existing literature on Coronavirus modelling research, covering both international and Japanese studies (Sec. 2). Next, in the data and methodology section (Sec. 3), we explore the four key considerations and elaborate on our research methodology. Following that, in the model construction section (Sec. 4), we explain how the model was developed. Then, in the verification and calibration phase (Sec. 5), we offer substantial evidence of the model's effectiveness, a long with a cautious calibration process. Subsequently, we conduct analysis and depict findings from simulations (Sec. 6). Finally, we summarize recommendations and draw conclusions (Sec. 7).

## 2 LITERATURE REVIEW

### 2.1 A Review of International Research

To provide a comprehensive overview, this literature review begins by examining the current state of international research in the field.

Purkayastha and colleagues compare the simulation results among five epidemiological models for transmission of SARS-CoV-2 in India (Purkayastha et al., 2021). According to their research, SEIR-FANSY model outperforms others by having the highest certainty in terms of width of 95% credible interval. Still their research fails to capture the government interventions or citizen's behavioural changes. While policies like lockdown across India did play an unignorable role in epidemic spreads.

Chadi and others pointed out the problems of vaccine distribution, whether to prioritize vaccinating those who had received the first dose or those who had never vaccinated (Saad-Roy et al., 2021). Despite the controversy surrounding this approach, many jurisdictions have decided to proceed with the delayed second dose strategy. This has resulted in a significant increase in the number of people who have been vaccinated. Researchers, however, argue that one-dose strategies may be effective in the short term,

but may not be the best approach in the long term if they do not account for immune robustness. Their study serves as inspiration to properly ensure the vaccination rate of the second dose when conducting vaccination simulations.

Hoertel and others build a stochastic ABM model based on real-world data, including information on the demographics of the French population, the transmission dynamics of the virus, and the effectiveness of various NPIs (Hoertel et al., 2020). The model was applied to simulate the spread of the disease under different scenarios, including the implementation of different NPIs such as social distancing, mask wearing, and contact tracing. Their model is well calibrated and validated with a Pearson's R value of 0.99 for ICU-bed occupancy as well as cumulative mortality. One of the limitations of their research is not considering the decline of antibodies which an individual acquires through either recovery or vaccination.

Cai and his team developed an age-structured stochastic compartmental susceptible-latent-infectious-removed-susceptible model to simulate transmission of SARS-CoV-2 Omicron in China (Cai et al., 2022). Furthermore, their model takes into account specific data on vaccine coverage among different age groups, the effectiveness of vaccines against various clinical outcomes, the gradual decline of immune protection over time, the utilization of diverse antiviral therapies, and the implementation of nonpharmaceutical interventions. Nonetheless, the mortality rate was assumed to remain constant over the projection period, while it actually depends on multiple factors such as virulence and medical resources.

### 2.2 A Review of Japanese Research

To delve deeper into the subject matter, the literature review then shifts focus to research conducted by Japanese scholars.

Chiba outlines strategies for controlling the spread of epidemics in Japan, focusing on mobility restrictions, reduced restaurant operating hours, and remote work (Chiba, 2021).

Yamauchi et al. investigate the relationship between epidemic trends, governmental interventions, and daytime population density in Tokyo. Their findings indicate a positive correlation between increased contact opportunities and higher infection rates (Yamauchi et al., 2022).

Murakami et al. employ agent-based modelling and GPS analysis to simulate the spread and containment of infections in Tokyo. Their research

underscores the significance of city-wide lockdowns and preventive measures in service establishments (Murakami et al., 2022).

While several studies have contributed valuable insights into the transmission dynamics and control strategies of COVID-19, there are still important research gaps that need to be addressed, such as the absence of simulation models that incorporate antibody decline on an individual level, the lack of consideration for the impact of declining immunity due to recovery or vaccination, and the need to explore optimal vaccination strategies. Furthermore, existing research often fails to capture the oscillatory growth and decay behavior of the virus incidence curve, particularly in terms of the subsequent waves after the initial outbreak. This limitation in predictability is particularly relevant given the observation that the number of confirmed patients in the eight epidemic waves in the Tokyo were only the tip of the iceberg. Difference in prediction and observation suggests a need for more comprehensive modelling approaches. Moreover, the literature review reveals that previous studies have not fully accounted for the interplay between government interventions, citizen behavioral changes, and the dynamics of virus transmission. Understanding the role of government policies and individual behaviors in the spread of the virus is crucial for designing effective control measures.

To address all these research gaps, this study aims to explain the eight epidemic waves in the Tokyo using agent-based modelling and an extended SEIR denotation. By incorporating the dynamics of antibody decline on an individual level and considering factors such as vaccination, virus mutation, government policy, and PCR test, this research seeks to provide a more comprehensive understanding of the transmission dynamics and control strategies for COVID-19 in the Tokyo area.

# 3 DATA AND METHODOLOGY

## 3.1 Data Collection

We conducted a preliminary examination of the four proposed factors using publicly available data and information from the Tokyo Metropolitan website. All the gathered data and information are utilized in the model development outlined in Sec. 4.

### 3.1.1 Vaccination

It is clear that mass vaccination plays a crucial role in decreasing the severity and mortality rates (Larrauri et al., 2022). Table 2 provides an overview of the five vaccination rounds conducted in Tokyo.

Table 2: Timeline of vaccination rounds in Tokyo and vaccination rates as of Nov. 30, 2022.

| Vaccination round | Starting Date | Interval between doses | Vaccination rate |
|---|---|---|---|
| 1st | 2021.04.12 | Not applicable | 78.1% |
| 2nd | 2021.05.03 | 3~8 weeks | 77.5% |
| 3rd | 2021.12.01 | 6~7 months | 65.7% |
| 4th | 2022.05.25 | 5~6 months | 80.4% for the elderly |
| Bivalent | 2022.09.20 | 3 months | - |

Table 3: Timeline of mutated variants first detected in Tokyo and the relative severe rates.

| Date | Events | Severe rate[1] |
|---|---|---|
| 2020.01.24 | 1st COVID-19 case detected | 23.81% |
| 2021.01.12 | 1st Gamma case detected | 0.76% |
| 2021.04.20 | 1st Delta case detected | 1.00% |
| 2021.08.31 | 1st Delta N501S case detected | 0.84% |
| 2021.11.30 | 1st Omicron case detected | 3.57% |
| 2021.12.25 (Approx.) | 1st Omicron BA.2 case detected | 0.56% |
| 2022.04.12 | 1st Omicron XE case detected | 0.02% |
| 2022.04.22 | 1st Omicron BA.4 case detected | 0.02% |
| 2022.04.29 | 1st Omicron BA.5 case detected | 0.02% |
| 2022.07.13 | 1st Omicron BA.2.75 case detected | 0.05% |
| 2022.07-2022.10 (Approx.) | 1st Omicron BA.4.6 case detected 1st Omicron BF.7 case detected 1st Omicron BN.1 case detected 1st Omicron BQ.1 case detected 1st Omicron BQ1.1 case detected | 0.02% ~0.06% |
| 2022.10.28 | 1st Omicron XBB case detected | 0.01% |

---

[1]   Severe rate = The number of severe patients receiving medical treatment/ The number of confirmed patients.

### 3.1.2 Virus Mutation

Table 3 provides an overview of the initial detection dates of notable mutated viruses in Japan, alongside their corresponding severity rates. As depicted in Table 3, there is an observable trend indicating a decrease in virus lethality.

### 3.1.3 Government Policy

When examining governmental measures, this paper highlights municipal governance, healthcare interventions, border controls, and preventative measures related to the Olympics. The Tokyo Metropolitan Government implemented seven states of emergency, as detailed in Table 4. While standard regulations were enforced during four of these emergencies, the remaining three saw relaxed regulations. Additionally, Tokyo adopted Highly Active Antiretroviral Therapy (HAART Therapy) for COVID-19 treatment starting July 19, 2021 (Table 5).

Table 4: Timeline of state of emergency/ quasi-state of emergency in Tokyo.

| Events | Duration |
|---|---|
| 1st wave state of emergency | 2020.04.07~2020.05.25 |
| 2nd wave state of emergency | 2021.01.08~2021.03.21 |
| 1st wave quasi-state of emergency | 2021.04.12~2021.04.24 |
| 3rd wave state of emergency | 2021.04.25~2021.06.20 |
| 2nd wave quasi-state of emergency | 2021.06.21~2021.07.11 |
| 4th wave state of emergency | 2021.07.12~2021.09.30 |
| 3rd wave quasi-state of emergency | 2022.01.21~2022.03.21 |

Table 5: Government approved COVID-19 therapies and relevant death rates of the confirmed cases.

| Therapies | Duration | Death% |
|---|---|---|
| Before HAART Therapy | 2020.01.26 ~ 2021.07.18 | 1.2% |
| HAART Therapy applied | 2021.07.19 ~ 2021.12.23 | 0.45% |
| Lagevrio and Paxlovid | 2021.12.24 ~ 2022.11.27 | 0.10% |
| Distribution of 'Xocova' | 2022.11.28 ~ 2023.01.02 | 0.001% |

The Ministry of Health, Labour and Welfare of Japan authorized the emergency use of Shionogi's oral medication, 'Xocova,' for COVID-19 treatment on November 22, 2022 (Matsuyama, 2022). Distribution of 'Xocova' commenced on November

28, 2022, benefiting approximately 1 million citizens. This development contributed to a further decrease in the severity and mortality rates (refer to Table. 5).

Regarding border measures, Japan briefly opened its borders to foreign residents twice in 2020. Since Oct 11, 2022, Japan has ceased border operations, fully reopening its border to independent travellers with no daily cap.

Japan held the Tokyo Olympics from July 23 to August 8, 2021. The first Olympic team arrived in Japan on June 1, 2021 (Zhang, 2021). Athletes were required to depart within 48 hours of completing their events (International_Olympic_Committee, 2021), implying a departure period from July 25 to August 10, 2021. Approximately 79,000 individuals travelled to Japan for the Tokyo Olympics (McCurry, 2021).

### 3.1.4 PCR Test

The PCR (Polymerase Chain Reaction) test detects genetic material from specific pathogens and is widely used for diagnosing COVID-19. In Tokyo, PCR testing is conducted either by medical institutions or health centers, with the latter primarily responsible for conducting major inspections. Typically, Tokyo residents undergo PCR testing on a voluntary basis, following the advice of their physicians and assessing their own health conditions. Criticism regarding the shortage of PCR testing capacity has been persistent.

As of March 6, 2022, PCR testing has been covered by medical insurance. This allows medical facilities to directly solicit tests from private testing institutes and other entities. Additionally, with insurance coverage approval for the antigen detection kit "Lumipulse SARS-CoV-2 Ag", saliva-based tests were accessible to asymptomatic patients from July 17, 2022 (MHLW, 2023b). Moreover, residents can opt to register on the Tokyo Metropolitan Government website to receive a complimentary antigen test kit delivered to their home if they believe they have symptoms or have been in close contact with an infected individual. This measure helps alleviate the burden on medical facilities for testing and consultations. In the event of a positive antigen test result, the individual can promptly begin a 14-day self-quarantine to mitigate further transmission of the infection.

### 3.1.5 Other Considerations

Another aspect taken into account in this study is school breaks. During winter, spring, and summer vacations, students tend to travel longer distances compared to regular term periods.

## 3.2 Methodology Discussion

### 3.2.1 Agent-Based Modelling

In this research, we utilize NetLogo (Wilensky, 1999), a beautiful agent-based modelling (ABM) software, to simulate the dynamics of the epidemic. The rationale behind this choice is rooted in ABM's ability to capture the nuanced individual heterogeneity within complex environments. When studying large-scale epidemic phenomena, it's crucial to account for variations in individual attributes due to the significant social and physical interactions among them. ABM can be fine-tuned by adjusting model parameters to ensure that the calculated R0 aligns with real-world measurements.

### 3.2.2 Extended SEIR Denotation

Our model incorporates individual health statuses, drawing inspiration from the SEIR model (Hethcote, 2000), while also introducing additional statuses such as 'Vaccinated' and 'Dead', enhancing the precision of health status description (Refer to Table 1).

# 4 MODEL CONSTRUCTION

## 4.1 Space and Population

A total of 13,920,000 individuals reside in Tokyo, resulting in a population density of 6,264 individuals per square kilometre (Statistics Bureau of Japan, 2021). The city has approximately 7,291 hospital beds in total. Assuming uniform distribution of static properties (such as infrastructure) and identical distribution of dynamic properties (such as population movement) throughout Tokyo city, our approach involves constructing a rectangular block measuring 2 kilometres in length, designed to mimic the geometry of the Tokyo area. Epidemic dynamics are simulated within this block using downscaled population and infrastructure figures. Refer to Fig 1 for further details.

By applying the aforementioned uniformity assumptions, the entire Tokyo region, comprising 23 municipalities, is linearly downscaled into a rectangular block measuring 2 kilometres in length and 1 kilometre in width. It should be emphasized that the population density and hospital's capacity depicted in Fig. 1 correspond to actual data. The adjusted count of entries and exits to and from a block fluctuates with each time interval in response to governmental directives and incoming and outgoing data.
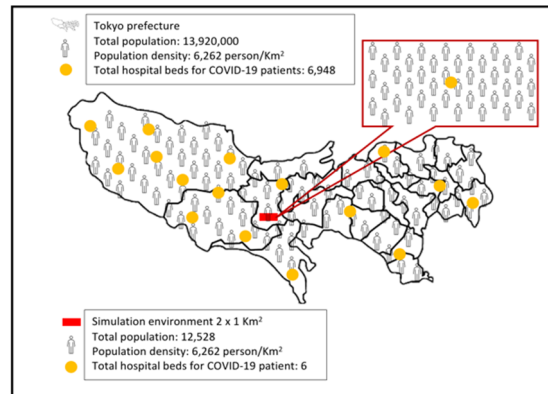


Figure 1: Illustration of post-scaled simulation environment.

## 4.2 Social Contact

In the model, agents are initially distributed randomly, with their location recorded as their place of residence. We presume that at the start of each day, all agents, excluding the quarantined ones, have the freedom to roam outdoors randomly for up to 8 hours in any direction within a radius denoted as $r_{max}$. This range matches their typical daily activities and varies based on their identity (whether they are employed, students, or unemployed). During these random walks, agents have opportunities to encounter other pedestrians, potentially leading to infection transmission. At the end of the day, agents return to their designated residences.

Although the social contact model described in this paper may not fully account for individual interactions at a precise level, we expect that its collective results will closely mirror those observed in broader epidemic contexts. A similar principle is evident in the microscopic modelling of fluid dynamics: despite variations in the molecules and interaction potentials of distinctive fluids, large-scale flow dynamics adhere to the same governing equation. This concept is echoed by Wolfram in his book on complex systems (Wolfram & Gad-el-Hak, 2003), where he highlights that although the underlying rules may differ across systems, the overall outcomes remain consistent.

## 4.3 Detailed Model Construction

The comprehensive system flowchart is depicted in Fig 2. Initially, we establish the patches area, synthetic population, and central hospital. Subsequently, the model processes input data from a file, which includes various parameters such as the

daily vaccine capacity, number of daily entries and exits, daily quota for PCR tests, infection probability for three levels of social distancing, maximum daily travel distance for three occupational categories, and mortality rates associated with different virus variants.
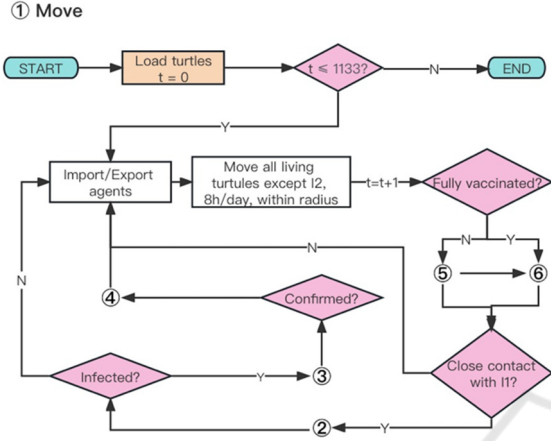
① Move



Figure 2: System flow chart of the simulation process.

Using published inbound and outbound traveler statistics, we introduce unconfirmed patients (represented as agents in category I1) and randomly export agents on a daily basis. Imported agents are also categorized based on their occupation. All surviving agents, with the exception of those in category I2, are permitted to move within specified distance boundaries corresponding to their respective occupations.

### 4.3.1 Health States and Population

We extend the SEIR categorization to encompass a total of eight health statuses for agents. (refer to Table 1). Furthermore, we segment the infected state into two subcategories, namely I1 and I2. Upon identification, confirmed cases (I2) are required to self-quarantine at home, thereby reducing their potential for public transmission compared to unconfirmed infected agents (I1). There are $N^{total}$ agents in this synthetic population. Among these agents, populations in different states are represented as $N^{S1}$, $N^{S2}$, $N^{E}$, $N^{I1}$, $N^{I2}$, $N^{V}$, $N^{R}$, $N^{D}$, respectively.

### 4.3.2 Susceptible

At the onset of the simulation (t=0), all agents are initially set to be susceptible (S1), with no individuals infected with the Coronavirus. Agents' home

positions are noted, and they are permitted to travel from their homes to locations within a designated radius denoted as $r_{max}$. Agents are allowed to venture out for a duration of eight hours daily, with movement unrestricted in direction. Upon reaching the boundary of the designated space, agents will rebound.

### 4.3.3 Exposure

Since the onset of imported cases spreading across the Tokyo on January 24, 2020, we designate this date as t=1. Over time, individuals who come into contact with asymptomatic cases (agents in state I1) have a chance of infection if they lack antibodies (see Fig. 3). The probability of transitioning from the Susceptible state to the Exposed state (S1→E) is calculated as follows:

$$P_{S1 \to E} = H(d_{S1,I1} - d_E) \tag{1}$$

Here, $H(x)$ represents the Heaviside step function, and $d_{X,Y}$ denotes the shortest distance between agents in state X and agents in state Y. The threshold distance, denoted as $d_E$, is set to 2 units of patch size, based on facts provided by the Ministry of Health, Labour, and Welfare, which states that physical proximity within 2 meters is considered close contact with a possibility of Coronavirus transmission (MHLW, 2023a).
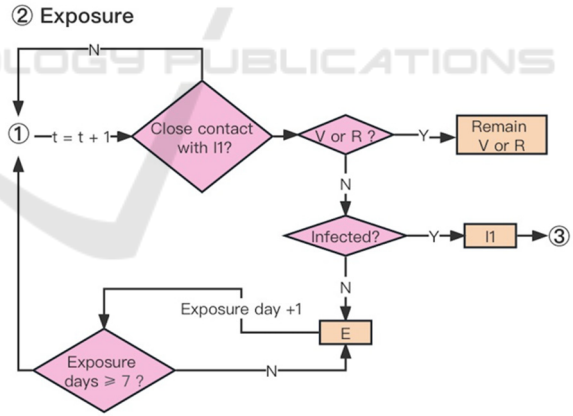
② Exposure



Figure 3: 'Exposure' in ABM.

### 4.3.4 Infection

Agents in state I1 have the potential to transmit Coronavirus to nearby agents (all surviving agents except for I1 and I2), exposing them to the virus within a specified distance. However, agents with antibodies above a certain threshold (in states V or R) cannot transition to the Exposed state (E). Exposed agents have a probability of developing symptoms and becoming infected within the subsequent 14 days.

The likelihood of an exposed agent (in state E) contracting Coronavirus relys on the distance at which the agent encountered another agent in state I1, as illustrated in Fig. 4.
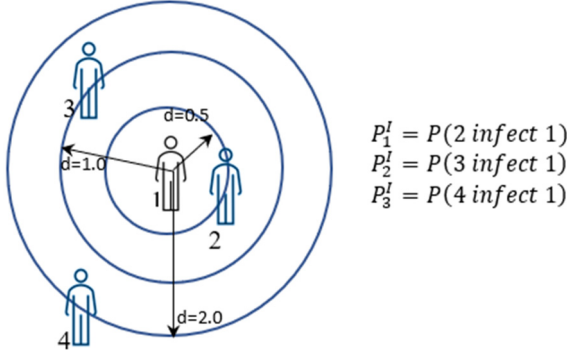


Figure 4: Illustration of agents' infection pattern.

The probability of infection ($P_{E \rightarrow I1}$) is defined as,

$$P_{E \rightarrow I1} = \begin{cases} P_1^I & 0 \leq d_{S1,I1} \leq 0.5 \\ P_2^I & 0.5 < d_{S1,I1} \leq 1.0 \\ P_3^I & 1.0 < d_{S1,I1} \leq 2.0 \end{cases} \quad (2)$$

Whenever the virus undergoes mutation, the probabilities of infection are adjusted based on the characteristics of the viruses. If exposed agents are fortunate enough to avoid infection, their states will revert back to S1 (E→S1). All agents, except the ones confirmed with infection (in state I2), will undergo PCR tests with a probability denoted as $P^T = n_T / (N^{total} - N^{I2} - N^D)$ per day, where $n_T$ represents the data of downscaled PCR tests released by the Tokyo Metropolitan Government. Upon confirmation of infectivity through PCR tests, the I1 state agents will be reclassified as I2 state (see Fig. 5). This implies that the transition probability for an individual can be computed as follows:

$$P_{I1 \rightarrow I2} = \frac{P^T \times N^{I1}}{N^{total} - N^{I2} - N^D}. \quad (3)$$

If an agent is currently in I2 state, movement shall be restricted until the subsequent state transition occurs, either to R (recovery) or D (death).

### 4.3.5 Recovery or Death

Agents testing positive for Coronavirus (in state I2) immediately begin a 14-day self-quarantine. Some may be hospitalized if beds are available, reducing mortality rates compared to home isolation. If not confirmed within 14 days, infected agents (in state I1) may move freely until recovery (I1→R) or death (I1 → D). Deceased agents are removed from the

simulation, while recovered agents gain antibodies and resume movement (see Fig. 6).

### 4.3.6 Vaccination

The daily vaccine supply quota prioritizes individuals for their second dose within three to seven weeks, with subsequent doses spaced accordingly (Fig. 7). All surviving individuals except confirmed, are eligible for vaccination while quotas last. Pfizer vaccine efficacy, estimated at 52% for the first dose and 91% for the second (Polack et al., 2020), is modelled despite vaccine brand options. Our model accounts for antibody titer decay, a factor often overlooked in existing literature.
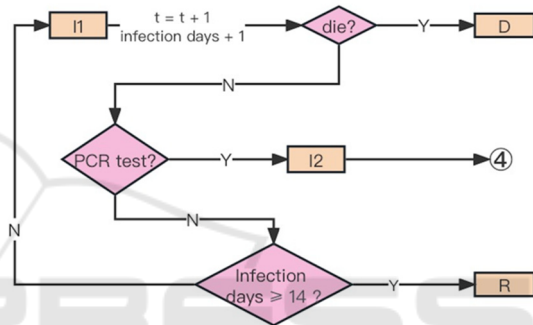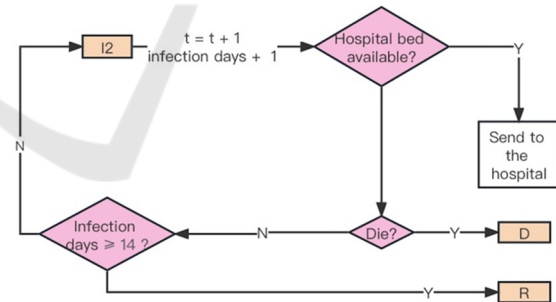


Figure 5: 'Infection' in ABM.



Figure 6: 'Confirmation' in ABM.

### 4.3.7 Antibody Decline

Antibodies are gained via vaccination or recovery, with natural recovery showing slower decline rates (Israel et al., 2022). The IgG test measures COVID-19 antibodies, with Narasimhan et al. setting a positive threshold at 50 AU/mL (Narasimhan et al., 2021), while Ebinger et al. suggest 4160 AU/mL for serum neutralizing activity (Ebinger et al., 2021).

In our model, individual antibody levels decrease over time based on previous studies. Once levels drop below a calibrated threshold, individuals transition to S2 status (V/R→S2).
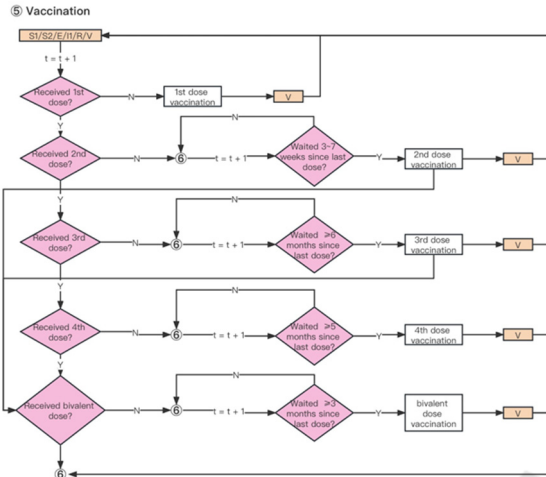


Figure 7: 'Vaccination' in ABM.

As per Ariel Israel et al., recipients of the Pfizer-BioNTech mRNA vaccine exhibit varying antibody levels compared to those who contracted the SARS-CoV-2 virus (see Fig. 8). Antibody concentrations gained via vaccination are initially higher but decline at a quicker pace (Israel et al., 2022).
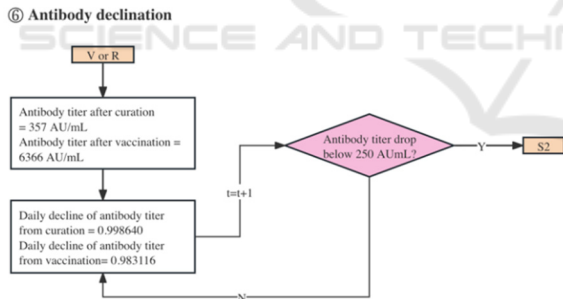


Figure 8: 'Antibody decline' in ABM.

# 5 VERIFICATION AND CALIBRATION

## 5.1 Verification of Linear Scaling

In Sec 4.1, Tokyo is downscaled into a 2km by 1km block, accommodating 12,528 susceptible agents and a hospital for 6 infected agents. We use a factor $\lambda < 1$ to demonstrated that simulation results can be scaled back to the real Tokyo scale post-simulation. Specifically, we designed four sizes of simulation

environments along with adjusted parameters $S_L : S_M : S_S : S_{XS} = 4 : 1 : (1/4) : (1/16)$. Test results from simulation show that the following relation holds true $N_L^{I2}/4 = N_M^{I2} = 4N_S^{I2} = 16N_{XS}^{I2}$, therefore $N^{I2}(\lambda S, \lambda N^{total}; t) = \lambda N^{I2}(S, N^{total}; t)$.

Moreover, the shape of the simulation area has trivial impact to results. Hence, we are confident to proceed the current model to perform simulations.

## 5.2 Calibration of the Model

To fine-tune this model, we utilize data on confirmed infection cases spanning from January 24, 2020, to May 8, 2023. Initial parameters like hospital capacity and population size are established within the code's initialization module (See Table 6).

Table 6: Parameters and parameter values.

| Parameters | Value | Parameters | Value |
|---|---|---|---|
| Initial population | 12,528 | Antibody titer after cured | 357 AU/mL |
| Hospital capacity | 6 | Decline rate for vaccinated | 0.980916 |
| Labor force participation rate | 62% | Decline rate for cured | 0.998640 |
| Student rate | 17% | Vaccine efficacy threshold | 250 AU/mL |
| 1st dose efficacy | 52% | Vaccination fatality rate | $8.1 \times 10^{-6}$ |
| 2nd dose efficacy | 91% | Self-isolation days | 14 days |
| Antibody titer 2nd dose | 1,629 | 1st/ 2nd dose Interval | 21~49 days |
| Antibody titer 3rd dose | 3,419 | 2nd/ 3rd dose Interval | $\geqq$180 days |
| Antibody titer 4th dose | 3,655 | 3rd/4th dose Interval | $\geqq$150 days |
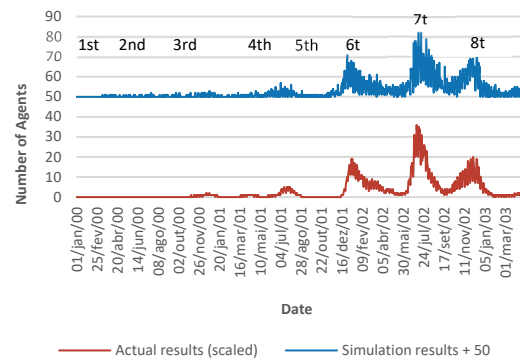


Figure 9: Actual results (scaled) vs. Simulation results.

# 6 ANALYSIS AND FINDINGS

## 6.1 Reproducing the Eight Waves

Fig. 9 compares scaled actual data with simulated daily COVID-19 infections in Tokyo from January 24, 2020, to May 8, 2023. The simulation, averaged over 60 iterations, successfully replicates the seven infection waves in Tokyo and predicts the highest daily confirmed cases in each wave, detailed in Table 7.

Table 7: Comparison of the maximum value between post-scaled actual results and simulation results.

| Epidemic waves in Tokyo | Maximum daily confirmed cases (post-scaling) | Maximum daily confirmed cases (simulation results) |
|---|---|---|
| 1st wave | 0 (April 27, 2020) | 0 (April 14, 2020) |
| 2nd wave | 0 (August 1, 2020) | 1 (August 1, 2020) |
| 3rd wave | 2 (January 7, 2021) | 1 (January 7, 2021) |
| 4th wave | 1 (May 8, 2021) | 2 (May 17, 2021) |
| 5th wave | 5 (August 13, 2021) | 4 (August 11, 2021) |
| 6th wave | 19 (February 2, 2022) | 19 (January 24, 2022) |
| 7th wave | 36 (July 28, 2022) | 33 (August 1, 2022) |
| 8th wave | 20 (December 27, 2022) | 19 (December 27, 2022) |

## 6.2 Analysis of Metrics

Fig. 10 depicts the scatter plot alongside marginal density and histogram, generated using 'ggscatterstats' function in the package 'ggstatsplot' (Patil, 2021). The number of observations $n_{pairs} = 1201$ corresponds to $2020.01.24 \sim 2023.05.08$.

The graph demonstrates a significant rejection of the null hypothesis with $p = 0.00 < 0.05$. The rejection is support by $\hat{r}_{Pearson} = 0.89$, which lies in $CI_{95\%}[0.88, 0.90]$. Overall, the statistical analysis indicates a strong agreement between the simulation results and actual data.

Furthermore, Granger causality tests were conducted on the two datasets. The F test statistic yielded a value of 64.008, with a corresponding p-value of $Pr_{(>F)} = 2.2 \times 10^{-16} < 0.05$. Consequently, we reject the null hypothesis, suggesting that the simulation results effectively predict the actual outcomes.

Examining the accuracy of the forecasts, the RMSE of 2.57 signifies the average absolute magnitude of forecast errors. Additionally, the DA of 0.76 indicates that the forecasts correctly predicted

the direction of the actual values approximately 76% of the time.



Figure 10: 'ggstatsplot' of results comparison.

Table 8: Evaluation metrics obtained from the calculation of actual and simulated results.

| Evaluation metrics | Reference range | Desired value | Value |
|---|---|---|---|
| R-Pearson | [0,1] | Closer to 1 (strong positive linear relationship) | 0.89 |
| R-squared | [0,1] | Closer to 1 (more variance explained) | 0.79 |
| Root Mean Squared Error (RMSE) | [0,+∞) | Closer to 0 (minimized as much as possible) | 2.57 |
| Directional Accuracy (DA) | [0,1] | Closer to 1 (high proportion of correct predictions) | 0.76 |

## 6.3 Findings

### 6.3.1 The 'Hidden' Infections

Fig 11 illustrates the counts of agents in E, I1, and I2 states from January 24, 2020, to May 8, 2023. Fig 12 shows vaccination doses administered during the same period.

Observations reveal:

1. The rise in I1 population correlates with an increase in E population, indicating a positive infection loop. Waves 1 to 4 depend on individual recovery and antibody production, with underreported cases due to insufficient testing.
2. Coronavirus mutations lead to a convergence of E and I1 populations until the late 6th wave. The 4th dose vaccination campaign, starting on May 25, 2022, mitigates the rise in E cases.
3. Despite a decrease in I1 population post-7th wave, expanded PCR testing capacity results in reported cases exceeding previous waves.

The robust correlation observed between PCR tests and confirmed cases indicates that the reported cases represent only a fraction of actual infections.

## 6.3.2 Antibody from Vaccination and Cure

Following vaccination rollout, antibody levels surged rapidly across the community. By October 2021, effectiveness waned, but rebounded in January 2022 with the Omicron variant and third vaccine dose introduction.

Amid escalating transmission and virus mutations, antibody levels increased gradually. The timely fourth /bivalent dose introduction further elevated population antibody levels to record highs.

## 6.3.3 Reasons Behind the Eight Waves

We outline features of the infection trends in Tokyo in Table 9. Here are the factors contributing to these characteristics:

1. Tokyo commenced its first vaccine dose during the 4th wave, later than New York and London, rendering it susceptible to future mutations (Tokyo: April 12, 2021; New York: December 14, 2020; London: December 8, 2020).
2. Insufficient PCR testing capacity in waves 1-5 failed to accurately reflect infection trends.
3. Improved PCR testing during the Omicron-dominated 6th wave revealed historically high confirmed cases, despite reduced severity and mortality rates due to previous vaccination and self-recovery (Larrauri et al., 2022).
4. BA.2.75 variant, identified in the 7th & 8th wave, evades most antibodies, hindering control efforts even with high vaccination rates (Fig 11 & Fig 12). Increased PCR testing primarily led to higher daily confirmed cases without effectively curbing overall infection trends.

Table 9: Summary of the eight epidemic waves in Tokyo with key assumptions and result.

| Epidemic waves | Key assumptions | | | | Key results | | | |
|---|---|---|---|---|---|---|---|---|
| | Vaccination | Virus mutation | Government policies | Daily PCR tests | I1 | I2 | Vaccination antibody | Infection antibody |
| 1st wave (2020.01~ 2020.05) | / | 1st COVID-19 case (2020.01.24) | 1st state of emergency (2020.04.07~ 2020.05.25) | Low (ave. 500) | High | Low | / | Start to increase due to self-healing |
| 2nd wave (2020.05~ 2020.10) | / | / | Bans entry from 159 countries and regions (2020.08.28) | Low (ave. 3600) | Low | Low | / | Start to decrease due to antibody decline |
| 3rd wave (2020.10~ 2021.03) | / | 1st Gamma case (2021.01.12) | 2nd state of emergency (2021.01.07~2021.03.21) | Low (ave. 7900) | Low | Low | / | Stable due to limited infection |
| .4th wave (2021.03~ 2021.06) | 1st dose start (2021.04.12) 2nd dose start (2021.05.13) | 1st Delta case (2021.04.20) | 1st quasi state of emergency (2021.04.12~ 2021.04.24) 3rd state of emergency (2021.04.25~ 2021.06.20) | Low (ave. 8600) | Low | Low | Start to increase | Increase due to mass infection |
| 5th wave (2021.06~ 2021.10) | / | 1st Delta N501S (2021.08.31) | 2nd quasi state of emergency (2021.06.21~ 2021.07.11) 4th state of emergency (2021.07.12~ 2021.09.30) | Medium (ave. 11,100) | High | Low | Dose 1 and 2 effectiveness start to decrease due to antibody decline | Continue to increase |
| 6th wave (2021.12~ 2022.06) | 3th dose start (2021.12.01) 4th dose start (2022.05.25) | 1st Omicron case (2021.11.30) 1st Omicron BA.2 (Approx.2021.12.25) 1st Omicron XE (2022.04.12) 1st Omicron BA.4 (2022.04.22) 1st Omicron BA.5 (2022.04.29) | 3rd quasi state of emergency (2022.01.09~ 2022.03.21) Limited foreign travel groups, up to 20,000 daily (2022.06.01) | High (ave. 17,100) | High | Medium high | Dose 3 and 4 effectiveness start to increase due to booster doses vaccination | Previous antibodies become less protective faced with Omicron strains; Infection antibodies targeting Omicron strains start to increase. |
| 7th wave (2022.06~ 2022.09) | Bivalent dose start (2022.09.20) | 1st Omicron BA.2.75 (2022.07.13) 1st Omicron XBB (2022.10.28) | Allow short-term trips organized by travel agencies, up to 50,000 daily (2022.09.07) | High (ave. 23,500) | High | High | Dose 3 and dose 4 become less protective; Bivalent dose effectiveness start to increase |  |
| 8th wave (2022.10~ 2023.01) |  |  | Fully reopen (2022.10.11) | High (ave. 16,400) | High | Medium high |  |  |
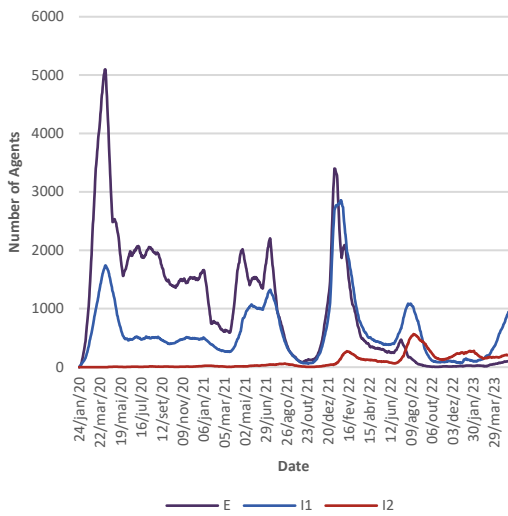
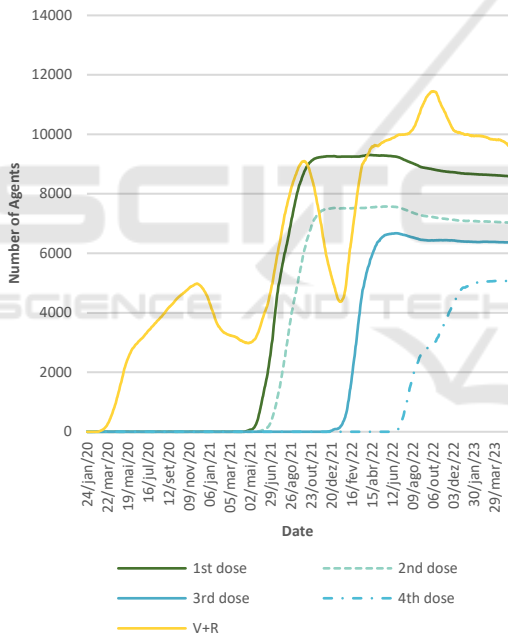Figure 11: Number of agents in E, I1 and I2 states.



Figure 12: 1st, 2nd, 3rd, 4th doses of vaccination.

# 7 RECOMMENDATION AND CONCLUSION

## 7.1 Recommendation

The decline in confirmed cases in late January led to a decrease in testing, indicating a reduced perception of infection risk among the public. This trend, known as the "testing dilemma," illustrates that fewer confirmed cases may result in decreased testing rates, potentially leading to fewer reported cases.

Report from The Japan News reveals a consistent rise in cases since April to May 2023. This surge may be attributed to the "testing dilemma." Moreover, cases continued to rise in June (Otake, 2023), with a significant increase in new patients reported.

To combat recurring outbreaks, it's crucial to maintain vigilance and promptly mobilize healthcare resources, including testing capabilities and hospital beds. Japan's opening-up policy must be monitored closely alongside daily confirmed cases, mutation detection, and fatality rates. Although fatality rates have decreased, the risk of new troublesome variants remains.

## 7.2 Conclusion

The resurgence of COVID-19 cases in late May and June highlights the importance of maintaining vigilance and mobilizing resources. Despite the low rates of severe cases and deaths, PCR tests may not significantly reduce infections but should be maintained to detect potential severe variants.

Tokyo's existing healthcare infrastructure is deemed satisfactory, taking into account the available hospital beds and anticipated low severe cases. However, the mobility to swiftly expand hospital bed capacity is imperative to manage potential outbreaks and imported mutated virus. High vaccination rates for third and fourth doses enhance immunity against Omicron variants, aligning closely with forecasted scenarios. A correlation exists between confirmed cases and testing levels, with fewer cases reported during reduced testing due to the "testing dilemma."

Novelty of this study lies in its demonstration of the importance of COVID-19 infection forecasting concerning vaccination, virus mutation, government policy, and PCR testing. It pioneers in continuously simulating and reproducing eight epidemic waves in Tokyo, considering factors like Olympics, state of emergency declarations, and immigration policies. The extension of the traditional SEIR model to adapt to Tokyo's context, along with an agent-based approach, ensures high accuracy and practicality. This model may serve as a general framework for analysing epidemics in other regions, emphasizing the importance of local considerations for better simulation results.

There are several flaws in this work. Firstly, this study focuses on four significant factors influencing epidemic trends but acknowledges that there are numerous other variables that may also impact these trends. While the theory of large-scale flow dynamics

is proposed to address agent movement, further refinement is needed to better represent real-world complexities. Additionally, demographic factors such as natural birth and death rates, as well as family dynamics, are not considered in this research, highlighting the need for future models to incorporate these elements. The simulation's strategy of randomly selecting agents for PCR tests diverges from real-world testing practices, which could affect the accuracy of results and should be addressed in future iterations. Lastly, the complexity of immune response, as highlighted by Dr. Israel, poses challenges in accurately incorporating antibody titer data into simulations due to individual variations and decay rates, emphasizing the importance of cautious interpretation in future studies.

## ACKNOWLEDGEMENTS

## REFERENCES

Cai, J., Deng, X., Yang, J., Sun, K., Liu, H., Chen, Z., . . . Zou, J. (2022). Modeling transmission of SARS-CoV-2 omicron in China. *Nature medicine*, *28*(7), 1468-1475.

Chiba, A. (2021). The effectiveness of mobility control, shortening of restaurants' opening hours, and working from home on control of COVID-19 spread in Japan. *Health Place*, *70*, 102622. https://doi.org/10.1016/j.healthplace.2021.102622

Chu, J., Morikawa, H., & Chen, Y. (2023). Simulation of SARS-CoV-2 epidemic trends in Tokyo considering vaccinations, virus mutations, government policies and PCR tests. *Biosci Trends*, *17*(1), 38-53. https://doi.org/10.5582/bst.2023.01012

Ebinger, J. E., Fert-Bober, J., Printsev, I., Wu, M., Sun, N., Prostko, J. C., . . . Braun, J. G. (2021). Antibody responses to the BNT162b2 mRNA vaccine in individuals previously infected with SARS-CoV-2. *Nature medicine*, *27*(6), 981-984.

Hethcote, H. W. (2000). The mathematics of infectious diseases. *SIAM review*, *42*(4), 599-653.

Hoertel, N., Blachier, M., Blanco, C., Olfson, M., Massetti, M., Rico, M. S., . . . Leleu, H. (2020). A stochastic agent-based model of the SARS-CoV-2 epidemic in France. *Nature medicine*, *26*(9), 1417-1421.

International_Olympic_Committee. (2021). *Tokyo 2020 Olympic Village(s) Period of stay Guidelines for the NOCs*. https://stillmedab.olympic.org/media/Document%20Library/OlympicOrg/News/2020/12/Tokyo-2020-Olympic-Village-Guidelines-for-NOCs-in-relation-to-period-of-stay-eng.pdf

Israel, A., Shenhar, Y., Green, I., Merzon, E., Golan-Cohen, A., Schäffer, A. A., . . . Magen, E. (2022). Large-scale study of antibody titer decay following BNT162b2 mRNA vaccine or SARS-CoV-2 infection. *Vaccines*, *10*(1), 64.

Larrauri, B., Malbran, A., & Larrauri, J. A. (2022). Omicron and vaccines: An analysis on the decline in COVID-19 mortality. *medRxiv*.

Matsuyama, K. (2022, 2022-11-22T21:22:33+09:00). *Shionogi COVID-19 pill Xocova wins emergency approval in Japan | The Japan Times*. @japantimes. Retrieved January 19, from https://www.japantimes.co.jp/news/2022/11/22/national/science-health/shionogi-covid-xocova-approval/

McCurry, J. (2021, 2021-05-20). *79,000 people flying in for Tokyo Olympics, Japanese media reports*. @guardian. Retrieved January 19, from http://www.theguardian.com/sport/2021/may/20/organisers-of-tokyo-olympics-press-ahead-despite-covid-fears

MHLW. (2023a). *COVID-19 Q&A*. Retrieved January 19, from https://www.mhlw.go.jp/stf/covid-19/qa.html

MHLW. (2023b). *COVID-19 tests*. Ministry of Health, Labour and Welfare. Retrieved January 19, from https://www.mhlw.go.jp/stf/seisakunitsuite/bunya/0000121431_00182.html

Murakami, T., Sakuragi, S., Deguchi, H., & Nakata, M. (2022). Agent-based model using GPS analysis for infection spread and inhibition mechanism of SARS-CoV-2 in Tokyo. *Sci Rep*, *12*(1), 20896. https://doi.org/10.1038/s41598-022-25480-z

Narasimhan, M., Mahimainathan, L., Araj, E., Clark, A. E., Markantonis, J., Green, A., . . . Fankhauser, K. (2021). Clinical evaluation of the Abbott Alinity SARS-CoV-2 spike-specific quantitative IgG and IgM assays among infected, recovered, and vaccinated groups. *Journal of clinical microbiology*, *59*(7), e00388-00321.

Otake, T. (2023). *COVID wave looms in Japan after case numbers nearly double in a month*. @japantimes.

Polack, F. P., Thomas, S. J., Kitchin, N., Absalon, J., Gurtman, A., Lockhart, S., . . . Group, C. C. T. (2020). Safety and Efficacy of the BNT162b2 mRNA Covid-19

Vaccine. *N Engl J Med*, *383*(27), 2603-2615. https://doi.org/10.1056/NEJMoa2034577

Purkayastha, S., Bhattacharyya, R., Bhaduri, R., Kundu, R., Gu, X., Salvatore, M., . . . Mukherjee, B. (2021). A comparison of five epidemiological models for transmission of SARS-CoV-2 in India. *BMC infectious diseases*, *21*(1), 1-23.

Saad-Roy, C. M., Morris, S. E., Metcalf, C. J. E., Mina, M. J., Baker, R. E., Farrar, J., . . . Levin, S. A. (2021). Epidemiological and evolutionary considerations of SARS-CoV-2 vaccine dosing regimes. *Science*, *372*(6540), 363-370.

Wilensky, U. (1999). NetLogo. Evanston, IL: Center for connected learning and computer-based modeling, Northwestern University. In.

Wolfram, S., & Gad-el-Hak, M. (2003). A new kind of science. *Appl. Mech. Rev.*, *56*(2), B18-B19.

Yamauchi, T., Takeuchi, S., Uchida, M., Saito, M., & Kokaze, A. (2022). The association between the dynamics of COVID-19, related measures, and daytime population in Tokyo. *Scientific Reports*, *12*(1), 1-12.

Zhang, Y. (2021, 2021-06-01). *Australia's softball players are among the first Olympic athletes to arrive in Japan. (Published 2021)*. @nytimes. Retrieved January 19, from https://www.nytimes.com/2021/06/01/world/asia/australia-olympics-tokyo-japan-softball.html